Experimental research of laser-induced periodic surface structures in a typical liquid by a femtosecond laser

Youwang Hu (胡友旺), Haoming Yue (岳浩铭), Ji'an Duan (段吉安), Cong Wang (王 聪), Jianying Zhou (周剑英), Yunpeng Lu (鲁云鹏), Kai Yin (银 恺), Xinran Dong (董欣然), Wenyi Su (苏文毅), and Xiaoyan Sun (孙小燕)*

State Key Laboratory of High Performance and Complex Manufacturing, College of Mechanical and Electrical Engineering, Central South University, Changsha 410083, China

**Corresponding author: sunxy@csu.edu.cn.*

Received August 25, 2016; accepted December 15, 2016; posted online January 12, 2017

A constant elastic alloy is a widely used material with a high elastic modulus and an excellent wave velocity consistency. Different morphologies on the constant elastic alloy surface are observed through femtosecond laser irradiation. When the laser average fluence is set to 0.58 J/cm^2 and 200 laser pulses, with the increasing depth of distilled water, the period of the laser-induced periodic surface structures (LIPSS) becomes shorter accordingly. The higher the ethanol concentration is, the more spot-shaped structures will be formed among the surface structures when the depth of the coverage of ethanol is 2 mm. The period of the LIPSS reaches its maximum when the concentration of ethanol is 80%.

OCIS codes: 320.2250, 220.4241, 100.0118.
doi: 10.3788/COL201715.021404.

Laser-induced periodic surface structures (LIPSS) are formed when a femtosecond laser radiates materials[1]. It is generally accepted that these LIPSS are generated by interaction of the incident laser beam with the surface electromagnetic wave (SEW). They are usually generated on surfaces by the excitation of surface plasmon polaritons (SPPs)[2]. The growth of LIPSS remains a point of discussion of many researchers[2–8]. Various research reported in the literature are using ultra-short pulse lasers to generate periodic structures on a variety of materials such as semiconductors[9,10], metals[11,12], and dielectrics[13]. The processing parameters of a femtosecond laser include wavelength, number of pulses, fluences, pulse duration, incident angles, and polarization. The effects of these parameters have been investigated on the spatial wavelength and depth of periodic surface structure of LIPSS[14]. Most of the previous studies on the LIPSS focus on those structures generated with the assistance of gaseous conditions. In recent years, some researchers have been studying LIPSS that are generated with the assistance of various liquids[15,16]. Interactions between the laser and the material in the liquid are considerably complicated, involving a highly confined plasma pressure, efficient cooling, enhanced chemical reactivity, and the generation of elevated temperatures, etc.[17–19]. Compared with LIPSS formed in gaseous environments, LIPSS fabricated in liquid conditions is more significant as it has an important application such as controlling generations of nanostructure and synthesis of nanoparticles.

According to previous research, the spatial wavelength of LIPSS in an atmospheric environment is generally longer than that in a liquid[14]. Different parameters, such as pulse width, wave length, fluence, numbers of pulses, the kind and depth of the liquids, the surfactant, and the nature of the target material have a great influence on liquid assisted laser ablation. These parameters can be taken as controlling during the processes of melting, evaporation, plasma generation, and generate nanostructures on the ablated surface[3]. However, few researchers have paid attention to the effect of different depths of distilled water and different concentrations of ethanol on LIPSS[3,14].

In this study, a constant elastic alloy was used to study the effect of the different femtosecond laser average fluences on the periodic surface structure. Experimental results show how the depths of distilled water, the laser average fluence, and the concentration of ethanol influence the periodical surface structures. It can provide some ways on how to employ better femtosecond laser parameters and an ablation medium to control the periodical surface structures.

The schematic of the experimental setup is shown in Fig. 1. A Ti:sapphire solid femtosecond laser from Spectra Physics Company is employed in these experiments. The maximum single pulse energy of the laser output by the

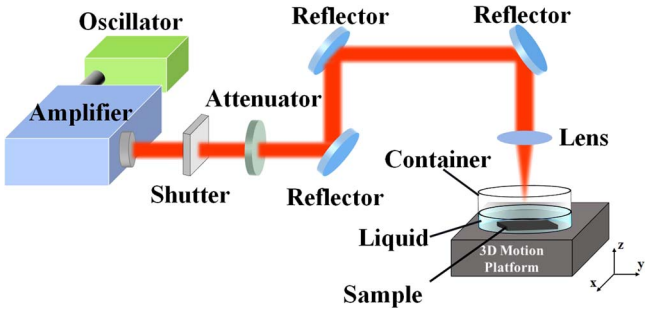

Fig. 1. Schematic diagram of the experimental setup.

femtosecond laser amplifier is 4 mJ. The wave width of output laser center is 800 nm. The minimum pulse width is 120 fs. The repetitive frequency is 1 kHz. The focal length of the focusing lens is 50 mm. The radius of the focus beam waist is 15.97 μm. In order to avoid the breakdown in liquids or other possible nonlinear optical effects covered on the sample surface, the focal point is set to 0.2 mm behind the sample surface after the sample is placed in the container without any liquids[16]. The container remains still while the liquid is being filled in the container in the following experiments. The samples used in our experiment have dimensions of 20 mm × 20 mm × 2 mm. The samples used in the experiments are made of a constant elastic alloy that has a chemical composition of 48.35% Fe, 42% Ni, 5.5% Cr, 2.5% Ti, 0.8% Mn, 0.8% Si, and 0.05% C[20]. After precision grinding and polishing, the surface roughness of the sample is about 0.1 μm. The sample in the container is installed on a 3D motion platform (Suruga, Inc.), which is controlled by a computer[20,21].

In the first part of the experiment, laser ablation under distilled water environments with different covering depths was carried out for comparisons. The depth of the liquid from the liquid surface to the sample top surface varied from 0.5 to 2.5 mm. In the second part, laser ablation was performed with different laser average fluences under the distilled water environment. The depth of the covering solution was fixed to 2 mm. In the third part, laser ablation in absolute ethanol with different depths was performed. Other conditions were identical to the first part. In the fourth part, samples were then ablated in ethanol with various concentrations; the epth of the ethanol was also fixed to 2 mm. The ethanol concentration varied from 0 to 100%. The number of laser pulses was 200 maintained for all ablations. After the laser processing, the samples were put in an ultrasonic bath cleaner with an ethanol rinse for 10 min to remove debris from the ablation process[14].

A scanning electron microscope (SEM) was employed to determine the surface morphology of the treated samples. Analyzing the results, the correlation between the periods of LIPSS and the covering depth of the distilled water or the concentration of ethanol solution was obtained.

Figure 2 shows the SEM images of the morphologies ablated in air and different depths of distilled water.

The surface structures were obtained with the laser average fluence set to 0.58 J/cm^2 and 200 laser pulses. The LIPSS were most distinct and defined when the depth is 2 mm. A clear dependence of the LIPSS period on the distilled water depths was acquired.

The arithmetic average of the spatial periods of each group is shown in Fig. 3. The points in the graph are fitted by two linear functions. It can be seen that the periods of the LIPSS ripples in the distilled water are lower than those in air. As shown in Fig. 2(b), when the depth of the liquid is 0.5 mm, the surface of the LIPSS break down, which may be because the threshold used for the surface modification in a liquid is lower than that in air[22]. As can

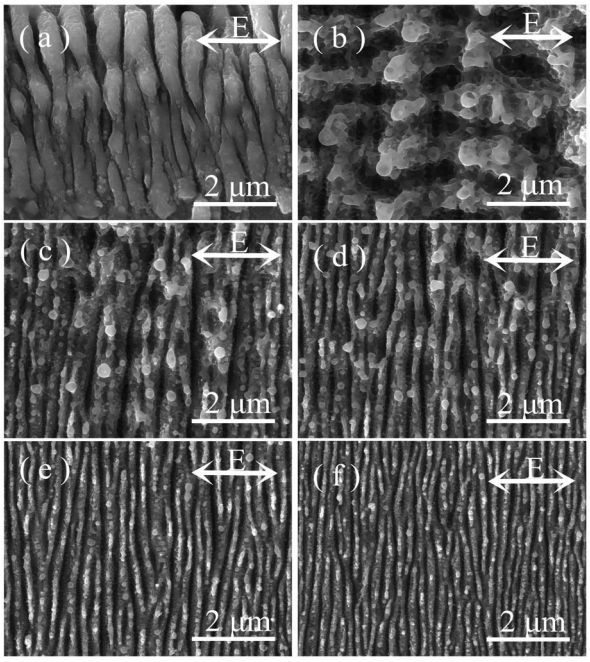

Fig. 2. LIPSS structures at the peripheral ablated area by a femtosecond laser under distilled water depths of: (a) 0, (b) 0.5, (c) 1, (d) 1.5, (e) 2, and (f) 2.5 mm.

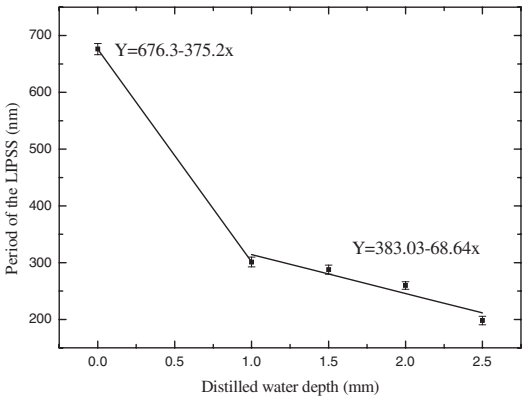

Fig. 3. Variation in the periods of LIPSS formed on a constant elastic alloy surface after femtosecond laser ablation under various distilled water depths.

be observed in Fig. 3, when the depth of the liquid is fixed at 1 mm, the period of the LIPSS in distilled water is 301.1 nm, which is about 53% less than that in air (676.3 nm). This result shows that the change in environmental medium plays an important role in the formation of LIPSS. As shown in Fig. 3, with the increasing depths of the liquid, the periods of the structures are decreasing. For example, the period of the structures in distilled water at a liquid thickness of 1.5 mm is 287.6 nm, while it is 198.1 nm at a liquid thickness of 2.5 mm. There is no LIPSS when the depth of thickness exceeds 2.5 mm. First, when the laser irradiates in liquid, the position of the theoretical laser focus will be located further below the sample surface with the increase of the depth of the liquid. As a result of

the decrease of the laser focus, the fluence of the laser ablated in the sample will fall down. Second, the thicker coverage has more restraint to laser-induced plasma, which leads to less material removal. Last, the increase of the liquid depth causes a higher loss of laser irradiating on the sample surface due to a higher absorption. These phenomena weaken the formation of LIPSS at the same time.

To acquire better LIPSS, the depth of coverage is set to 2 mm and the number of laser pulses is set to 200. As shown in Fig. 4, the laser fluence has a high influence on the surface structures. Cracks among surface structures are widened along with the increasing laser fluence. When the average fluences are 0.29 and 0.41 J/cm^2, as shown in Figs. 4(a) and 4(b), the LIPSS are small. As shown in Fig. 4(c), when the average fluence is 0.58 J/cm^2, the homogenity of LIPSS is better. The lines of LIPSS are parallel to each other and less lines have ruptured. When the laser average fluence increases to 0.70 J/cm^2, the LIPSS are also regular, but a few spot-shape structures exist, as shown in Fig. 4(d). When the laser average fluence increases to 0.87 J/cm^2, the LIPSS are less commensurable, as shown in Fig. 4(e). This is probably because laser fluence is higher than the ablation threshold of the sample. Therefore, the number of spot-shaped structures increases and the cracks of the surface structures widen. Such changes in surface structures lead to poor quality of the LIPSS.

Figure 5 shows that the arithmetic average of the spatial periods of ripples after ablation with various laser average fluences under the distilled water environment. The points in the graph are fitted by a linear function. The periods of LIPSS increase from 152 to 312 nm with increasing laser average fluences from 0.29 to 0.87 J/cm^2. When the laser average fluence increases to 0.87 J/cm^2, the surface structures become irregular and the periods of LIPSS reach their maximum, which is obvious in the plot of Fig. 5. The period of the structures increases with increasing laser fluence[23].

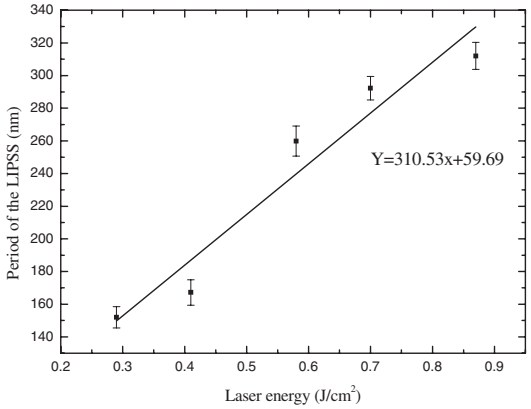

Fig. 5. Variation in the periods of LIPSS formed on a constant elastic alloy surface after femtosecond laser ablation for various laser average fluences in the distilled water environment.

Same experiments were carried out in absolute ethanol. The laser average fluence was set to 0.58 J/cm^2 and the number of laser pulses was 200. As shown in Fig. 6, different depths of ethanol influence greatly the surface structures when the process is done under the cover of absolute ethanol. The area of spot-shaped structures is becoming smaller when the depth of ethanol increases. The distances among these spot-shaped structures have an identical variation tendency with area. There is no commensurable LIPSS observed in absolute ethanol. Regular surface structures are hard to form in absolute ethanol.

To further investigate how liquid influences the period of LIPSS, experiments under the environment of various ethanol concentrations were carried out. The SEM images of the sample surfaces after laser processing in different

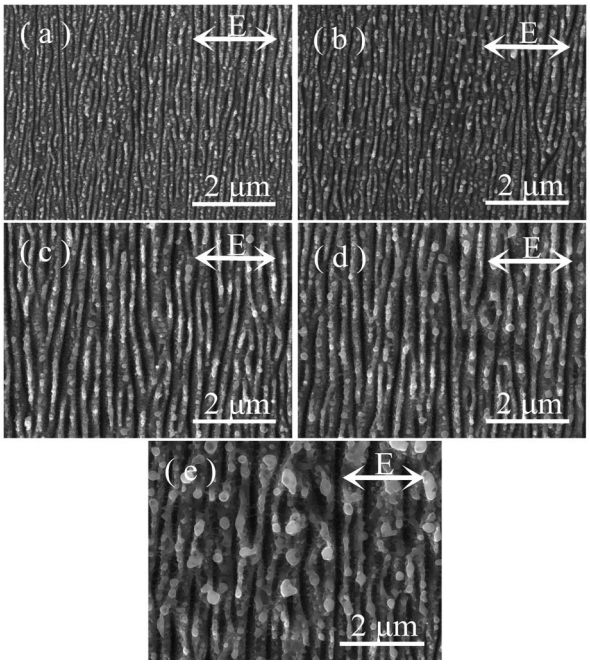

Fig. 4. LIPSS structures at the peripheral ablated area by a femtosecond laser with average fluences of: (a) 0.29, (b) 0.41, (c) 0.58, (d) 0.70, and (e) 0.87 J/cm^2.

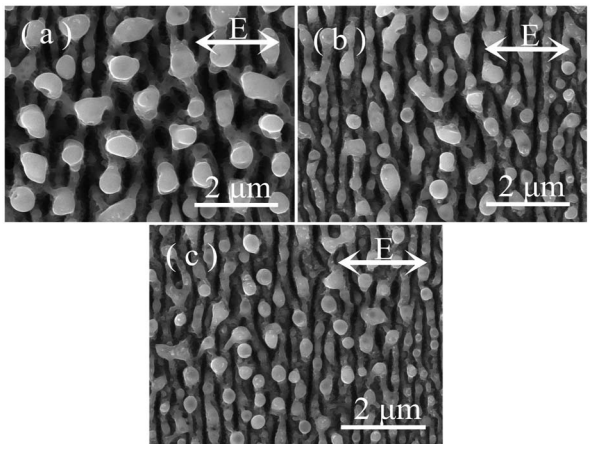

Fig. 6. LIPSS structures at the peripheral ablated area by a femtosecond laser under absolute ethanol depths of: (a) 1, (b) 2, and (c) 2.5 mm.

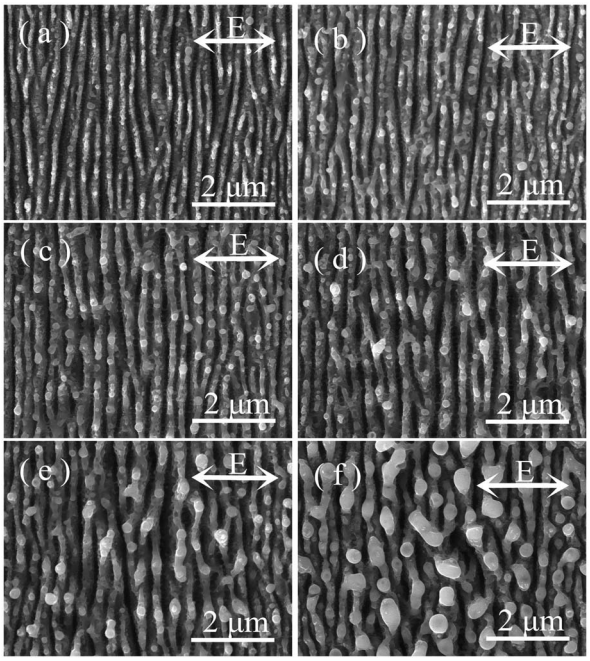

Fig. 7. LIPSS structures at the peripheral ablated area by a femtosecond laser in ethanol concentration environments of: (a) 0%, (b) 20%, (c) 40%, (d) 60%, (e) 80%, and (f) 100%.

ethanol concentrations are shown in Fig. 7. The laser average fluence and the number of laser pulse are identical to the values used in the aforementioned experiment. The depth of the coverage of ethanol was set to 2 mm. It can be seen from Fig. 7 that the ethanol concentration has a great influence on the formation of LIPSS. The spot-shaped structures on the surface are increasing with increasing ethanol concentration. The LIPSS are more commensurable when the concentration is 40%. When the ethanol concentration is 100%, it is difficult to form LIPSS on the surface of the sample.

The arithmetic average and standard errors of the spatial periods of each group in different ablated solutions are shown in Fig. 8. The points in the graph are fitted by a linear function. It can be seen that the periods of the structures in ethanol with different concentrations vary from

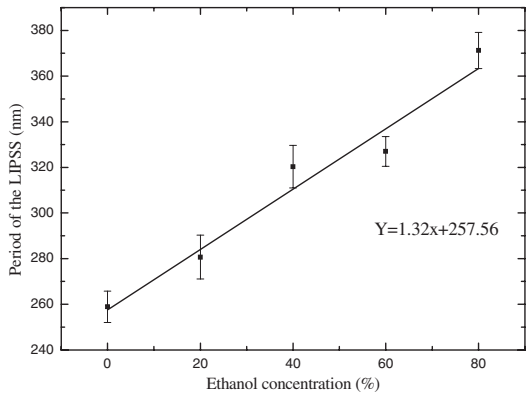

Fig. 8. Variation of the period of LIPSS formed on a constant elastic alloy surface after femtosecond laser ablation under various ethanol concentrations.

each other. With the increase of ethanol concentration, the period of the structures increases, reaching a peak when the ethanol concentration is 80%. There are no commensurable LIPSS observed in absolute ethanol. On the one hand, when the depth of the liquid is 2 mm, the laser focus will be closer to the target surface with the increase of refractive index, which increases with the increase of ethanol concentration[24]. On the other hand, the energy loss will increase along with the increase of the ethanol concentration, which is not as influential as the refractive index[25]. Under the combined effect of these two factors, the laser fluence at the sample surface increases with the increase of the ethanol concentration, which leads to an increased period of LIPSS.

This Letter analyzes and discusses the LIPSS induced by an 800 nm femtosecond laser on a constant elastic alloy in the conditions of air, distilled water, and ethanol. It is observed that the period of LIPSS structures decreases as the coverage of distilled water deepens. The period of the LIPSS structures becomes smaller with the increasing depths of the liquid. Periodic structures will not be formed when the depth of the coverage solution exceeds 2.5 mm. It is assumed that the coverage of liquid leads to a higher loss of laser energy. Thus, the fluence of the laser decreases with the increasing depth of the liquid. Meanwhile, the concentration of ethanol influences the period of the LIPSS. When the ethanol concentration is 80%, the period of the LIPSS is the largest. The higher the concentration of ethanol, the more spot-shaped structures are found on the surface. When the ethanol concentration is 100%, it is difficult to form LIPSS on the surface of the constant elastic alloy sample. The result will be a reference to get distinct and well-defined periodical surface structures on a constant elastic alloy with a femtosecond laser.

This work was supported by the National Natural Science Foundation of China (Nos. 51335011, 51475481, 51475482, and 91323301) and the Fundamental Research Funds for the Central Universities of Central South University.

References

1. P. E. Dyer and R. J. Farley, J. Appl. Phys. **2**, 74 (1993).
2. T. J. Y. Derrien, R. Koter, J. Krüger, S. Höhm, A. Rosenfeld, and J. Bonse, J. Appl. Phys. **116**, 074902 (2014).
3. S. Bashir, M. S. Rafique, and W. Husinsky, Nucl. Instrum. Methods B **275**, 1 (2015).
4. J. E. Sipe, J. F. Young, J. S. Preston, and H. M. Van Driel, Phys. Rev. B **27**, 1141 (1983).
5. F. Meng, J. Hu, W. Han, P. Liu, and Q. Wang, Chin. Opt. Lett. **13**, 062201 (2015).
6. T. Q. Jia, H. X. Chen, M. Huang, F. L. Zhao, J. R. Qiu, R. X. Li, Z. Z. Xu, X. K. He, J. Zhang, and H. Kuroda, Phys. Rev. B **72**, 125429 (2005).
7. X. Dong, H. Song, and S. Liu, Chin. Opt. Lett. **13**, 071001 (2015).
8. A. Y. Vorobyev, V. S. Makin, and C. Guo, J. Appl. Phys. **101**, 034903 (2007).
9. J. Bonse, A. Rosenfeld, and J. Kruger, J. Appl. Phys. **106**, 104901 (2009).

10. B. Gao, T. Chen, V. Khuat, J. Si, and X. Hou, Chin. Opt. Lett. **14**, 021407 (2016).
11. J. Wang and C. Guo, Appl. Phys. Lett. **87**, 2 (2005).
12. H. Song, Y. Zhang, X. Dong, and S. Liu, Chin. Opt. Lett. **14**, 123202 (2016).
13. X. C. Wang, G. C. Lim, W. Liu, C. B. Soh, and S. J. Chua, Appl. Surf. Sci. **252**, 2071 (2005).
14. L. S. Jiao, E. Y. K. Ng, and H. Y. Zheng, Appl. Surf. Sci. **264**, 52 (2013).
15. E. V. Barmina, E. Stratakis, M. Barberoglou, V. N. Stolyarov, I. N. Stolyarov, C. Fotakis, and G. A. Shafeev, Appl. Surf. Sci. **258**, 5898 (2012).
16. C. Albu, A. Dinescu, M. Filipescu, M. Ulmeanu, and M. Zamfirescu, Appl. Surf. Sci. **278**, 347 (2013).
17. L. J. Radziemski and D. A. Chemical, *Laser-Induced Plasmas and Applications* (Marcel Dekker Inc., 1989).
18. S. Bashir, M. S. Rafique, A. Ajami, W. Husinsky, and U. Kalsoom, Appl. Phys. A **113**, 673 (2013).
19. V. Kara and H. Kizil, Opt. Laser. Eng. **50**, 140 (2012).
20. L. S. Tan, H. L. Seet, M. H. Hong, and X. P. Li, J. Mater. Process. Technol. **209**, 4449 (2009).
21. A. De Bonis, T. Lovaglio, A. Galasso, A. Santagata, and R. Teghil, Appl. Surf. Sci. **353**, 433 (2015).
22. C. Wang, H. Huo, M. Johnson, M. Shen, and E. Mazur, Nanotechnology **21**, 075304 (2010).
23. Y. Shimotsuma, P. G. Kazansky, J. Qiu, and K. Hirao, Phys. Rev. Lett. **91**, 247405 (2003).
24. C. Wohlfarth, *Viscosity of the Mixture (1) Water; (2) Ethanol* (Springer, 2009).
25. H. W. Liu, F. Chen, X. H. Wang, Q. Yang, H. Bian, J. H. Si, and X. Hou, Thin Solid Films **518**, 5188 (2010).